Johann Radon Institute for
Computational and Applied Mathematics
Austrian Academy of Sciences (ÖAW)

ÖAW AUSTRIAN ACADEMY OF SCIENCES

RICAM
JOHANN·RADON·INSTITUTE
FOR COMPUTATIONAL AND APPLIED MATHEMATICS

Faithful Recovery of Vector Valued Functions from Incomplete Data. Recolorization and Art Restoration

M. Fornasier

RICAM-Report 2006-31

Faithful Recovery of Vector Valued Functions from Incomplete Data
Recolorization and Art Restoration

Massimo Fornasier[1]

Program in Applied and Computational Mathematics
Princeton University, Princeton NJ 08544, USA,
`mfornasi@math.princeton.edu`

Abstract. On March 11, 1944, the famous Eremitani Church in Padua (Italy) was destroyed in an Allied bombing along with the inestimable frescoes by Andrea Mantegna *et al.* contained in the Ovetari Chapel. In the last 60 years, several attempts have been made to restore the fresco fragments by traditional methods, but without much success. We have developed an efficient pattern recognition algorithm to map the original position and orientation of the fragments, based on comparisons with an old gray level image of the fresco prior to the damage. This innovative technique allowed for the partial reconstruction of the frescoes. Unfortunately, the surface covered by the fragments is only 77 m^2, while the original area was of several hundreds. This means that we can reconstruct only a fraction (less than 8%) of this inestimable artwork. In particular the original color of the blanks is not known. This begs the question of whether it is possible to estimate *mathematically* the original colors of the frescoes by making use of the potential information given by the available fragments and the gray level of the pictures taken before the damage. Can one estimate how *faithful* such restoration is? In this paper we retrace the development of the recovery of the frescoes as an inspiring and challenging real-life problem for the development of new mathematical methods. We introduce two models for the recovery of vector valued functions from incomplete data, with applications to the fresco recolorization problem. The models are based on the minimization of a functional which is formed by the discrepancy with respect to the data and additional regularization constraints. The latter refer to joint sparsity measures with respect to frame expansions for the first functional and functional total variation for the second. We establish the relations between these two models. As a byproduct we develop the basis of a theory of fidelity in color recovery, which is a crucial issue in art restoration and compression.

1 Introduction

Mathematical Imaging in Art Restoration. We address the problem of the faithful reconstruction of vector valued functions from incomplete data, with special emphasis in color image recovery. We are inspired by a real-life problem, *i.e.*

the rebirth of one of the most important masterpieces of the Italian Renaissance, by making use of mathematical imaging techniques. We refer to the decorative cycle in the Ovetari Chapel in the Eremitani Church in Padua. The chapel was seriously damaged by an air strike in 1944 and a large section of the contained frescoes were *sparsely* fragmented. A digital cataloging of pictures of the remain-
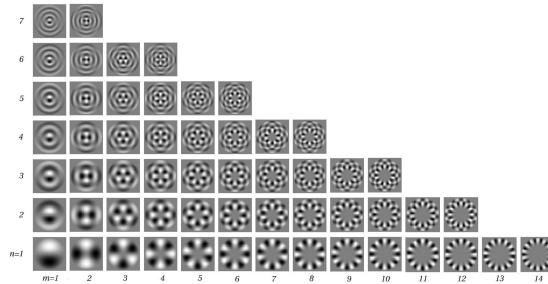

Fig. 1. Circular harmonic functions constitute an orthonormal basis of eigenfunctions of rotations. The comparison of two mutually rotated images amounts to the matching of the corresponding basis coefficients up to multiplication by suitable unitary eigenvalues.

ing fragments made it possible to count the number (78.561) of those with an area larger than 1 cm^2. The distribution of the areas shows that most of them are relatively small (5-6 cm^2). There is no information on the possible location of the pieces on the huge original surface and also unknown is the angle of rotation with respect to the original orientation. These *a priori* data demonstrated the lack of contiguous fragments for any given fragment.These difficulties explain the unsuccessful attempts of recomposition by traditional methods. In simple words, it is an incomplete *puzzle* which is too big to be solved by human eyes only. There exist some fairly good quality black and white photographs of the frescoes dated from between 1900 and 1920.This heritage gave rise to the hope that a computer-based comparison between the fresco digital images and those of the fragments could help to recognize their original location. The request of a fast algorithm excludes the implementation of comparisons *pixel-by-pixel* and suggests that methods based on compressed/sparse representations, *i.e.*, basis or frame expansions, can be more efficient. We have developed an efficient pattern recognition algorithm based on sparse *circular harmonic* expansions (Fig. 1) [20, 21]. This method has been implemented for the solution of the fragment recollocation problem and we illustrate some of the final results in Fig. 2. On the basis of the map produced by this *computer assisted anastylosis*, part of the frescoes has already been physically restored. We refer to the book chapter [8] for more details.

Even though the collocation of one single fragment is of historical and cultural importance, the success of the computer assisted anastylosis has been partially

spoiled by the limited surface that the fragments can cover. This begs the question of whether it is possible to estimate *mathematically* the original colors of the missing parts of the frescoes by making use of the potential information given by the available fragments and the gray level of the pictures taken before the damage. Can one estimate how *faithful* such restoration is?

Fig. 2. Fragmented A. Mantegna's frescoes (1452) by a bombing in the Second World War. Computer based reconstruction by using efficient pattern matching techniques [21].

Mathematical Inpainting and Recolorization. *Mathematical inpainting*, an artistic synonym for image interpolation, has been introduced by Sapiro et al. [3] with the specific purpose of imitating the basic approaches used by professional restorers when filling blanks in paintings. Their algorithm amounts to the solution of an evolutionary differential equation whose steady-state is the prolongation of the incomplete image in the inpainting region to make constant the information along isophotes. See also further recent developments [1]. Closely related to inpainting is the contribution by Masnou and Morel [25–27] who addressed the so-called *disocclusion problem*. Essentially it amounts to an application of the principle of *good continuation*, *i.e.*, without forming undesired T-junctions and abrupt direction changes, of the image level curves into the region where an occlusion occurred in order to restore the essential morphology. This work can be seen as a development of the theory of Euler's elastica curves by Mumford [28]. Chan and Shen contributed to inpainting with other models similar or related to the ones previously cited, see [9–13]. In simple words, mathematical inpainting is the attempt to guess the morphology of the image in a relatively small missing part from the level curves of the relevant known part. The recolorization problem, like that of the frescoes, can be viewed as a particular case of inpainting. Nevertheless, in this case two significant differences occur with respect to the classical problem: 1) The region of missing color is usually much larger than the one with known colors 2) the morphology of the image in the missing part can be determined by the known gray level, see also [7]. Several approaches to the recovery of colors in gray level images have been recently proposed based on different intuitions. Neighboring pixels with similar intensities

should have similar color. By using non-local fitting term an algorithm based on optimization has been proposed in [23] to match the colors. Similarly, a fast algorithm using a weighted distance image blending technique is studied in [31]. From the assumption that the color morphology is essentially determined by the gradient of the gray level, Sapiro proposed in [29] a recolorization method based on minimizing the difference between the gradient of gray level and the gradient of color. The problem reduces to the solution of a (nonlinear) boundary value problem. Based on similar assumptions two variational approaches are proposed in [22] where the authors minimize the discrepancy with respect to the color datum and impose a smoothness constraint on the solution out of the gray level discontinuity set. All the proposed solutions show that a very limited amount of color is sufficient information to recover a pleasant result. However none of these approaches seem to emphasize the problem of the *fidelity* of the recovered color.

The Fidelity of Restoration. Recolorization can be indeed a controversial practice, especially if we claim to "estimate" the color of an art masterpiece. It is therefore crucial to investigate the relations between amount of color data, model of reconstruction, and fidelity of the solution. Clearly this issue can also have a relevant role for color image compression.

In this paper we review two different approaches to recolorization previously proposed by the author *et al.* in [18, 19]. Since color images are modeled as multichannel signals, the problem is reformulated as the recovery of vector valued functions from incomplete data. The vector components are assumed to be coupled. The difference between the proposed methods is the way we couple the information. For both the approaches, the recovery is realized as the minimization of a functional which is formed by the discrepancy with respect to the data and additional regularization constraints. The latter refer to joint sparsity measures with respect to frame expansions for the first functional and functional total variation for the second. We establish the relations between these two models. As a byproduct we develop the basis of a corresponding theory of fidelity in color recovery.

2 Recovery of Vector Valued Data with Joint Sparsity Constraints

2.1 Sparse Frame Expansions

A *sparse representation* of an element of a Hilbert space is a series expansion with respect to an orthonormal basis or a frame that has only a small number of large coefficients. Several types of signals appearing in nature admit sparse frame expansions and thus, sparsity is a realistic assumption for a very large class of problems [24]. The recent observation that it is possible to reconstruct sparse signals from vastly incomplete information [6, 5, 15] stimulated a new fruitful line of research which is called *sparse recovery* or *compressed sensing*. This section is devoted to reveal the relations between faithful sparse recovery, vector valued functions, and the application to color images. Indeed multi-channel signals (i.e., vector valued functions) may not only possess sparse frame expansions

for each channel individually, but additionally the different channels can also exhibit common sparsity patterns. Color images are multi-channel signals, exhibiting a very rich morphology. In particular, discontinuities may appear in all the channels at the same locations. This will be reflected, *e.g.*, in sparse curvelet expansions [4, 16] with relevant coefficients appearing at the same labels, or in turn in sparse gradients with supports at the same locations.

2.2 Inverse Problems with Joint Sparsity Constraints

Let $\mathcal{K}$ and $\mathcal{H}_j$, $j = 1, \ldots, N$, be (separable) Hilbert spaces and $A_{\ell,j} : \mathcal{K} \to \mathcal{H}_j$, $j = 1, \ldots, M$, $\ell = 1, \ldots, N$, some bounded linear operators. Assume we are given data $g_j \in \mathcal{H}_j$, $g_j = \sum_{\ell=1}^{M} A_{\ell,j} f_\ell$, $j = 1, \ldots, N$. Then our basic task consists in reconstructing the (unknown) elements $f_\ell \in \mathcal{K}$, $\ell = 1, \ldots, M$. In practice, it happens that the corresponding mapping from the vector (f_ℓ) to the vector (g_j) is not invertible or ill-conditioned, as for the recolorization problem. In order to exploit sparsity ideas we assume that we have given a suitable frame $\{\psi_\lambda : \lambda \in \Lambda\} \subset \mathcal{K}$ indexed by a countable set Λ. This means that there exist constants $C_1, C_2 > 0$ such that $C_1 \|f\|_{\mathcal{K}}^2 \leq \sum_{\lambda \in \Lambda} |\langle f, \psi_\lambda \rangle|^2 \leq C_2 \|f\|_{\mathcal{K}}^2$, for all $f \in \mathcal{K}$. Orthonormal bases are particular examples of frames. Frames allow for a (stable) series expansion of any $f \in \mathcal{K}$ of the form $f = Fu := \sum_{\lambda \in \Lambda} u_\lambda \psi_\lambda$, where $u = (u_\lambda)_{\lambda \in \Lambda} \in \ell_2(\Lambda)$. Introduce the operators $T_{\ell,j} = A_{\ell,j} F : \ell_2(\Lambda) \to \mathcal{H}_\ell$ and

$$ T : \ell_2(\Lambda, \mathbb{R}^M) \to \mathcal{H}, \quad Tu = \left(\sum_{\ell=1}^{M} T_{\ell,j} u^\ell \right)_{j=1}^{N} = \left(\sum_{\ell=1}^{M} A_{\ell,j} F u^\ell \right)_{j=1}^{N}, $$

$u^\ell := (u_\lambda^\ell)_{\lambda \in \Lambda}$. We denote also $u_\lambda = (u_\lambda^\ell)^{\ell=1,\ldots,M}$, and $u = (u_\lambda^\ell)_{\lambda \in \Lambda}^{\ell=1,\ldots,M}$. Our recovery model [19] is based on the minimization of the functional

$$ J(u,v) = J_{\theta,\rho,\omega}^{(q)}(u,v) := \|Tu - g|\mathcal{H}\|^2 + \sum_{\lambda \in \Lambda} v_\lambda \|u_\lambda\|_q + \sum_{\lambda \in \Lambda} \omega_\lambda \|u_\lambda\|_2^2 + \sum_{\lambda \in \Lambda} \theta_\lambda (\rho_\lambda - v_\lambda)^2. \tag{1} $$

restricted to $v_\lambda \geq 0$. Here, $(\theta_\lambda)_\lambda$, $(\omega_\lambda)_\lambda$, and $(\rho_\lambda)_\lambda$ are some suitable positive sequences. The functional depends on two variables. The first belongs to the space of signal coefficients to be reconstructed, the second belongs to the space of sparsity indicator weights. We minimize $J(u,v)$ jointly with respect to both u, v. Analyzing $J(u,v)$ we realize that for the minimizer (u^*, v^*) we will have $v_\lambda^* = 0$ (or close to 0) if $\|u_\lambda^*\|_q = \left(\sum_{\ell=1}^{M} |u_\lambda^\ell|^q \right)^{1/q}$ is large so that $v_\lambda^* \|u_\lambda^*\|_q$ gets small. On the other hand, if $\|u_\lambda^*\|_q$ is small then the term $\theta_\lambda(\rho_\lambda - v_\lambda^*)$ dominates and forces v_λ^* to be close to ρ_λ. Moreover, for the parameter $q > 1$, the model imposes a further coupling of the sparsity pattern through different channels, see [19, 30]

The recovery algorithm consists in alternating a minimization with respect to u and a minimization with respect to v. More formally, for some initial choice

$v^{(0)}$, for example $v^{(0)} = (\rho_\lambda)_{\lambda \in \Lambda}$, we define

$$
\begin{aligned}
u^{(n)} &:= \arg\min_{u \in \ell_2(\Lambda,\mathbb{R}^M)} J(u, v^{(n-1)}), \\
v^{(n)} &:= \arg\min_{v \in \ell_{\infty,\rho^{-1}}(\Lambda)_+} J(u^{(n)}, v).
\end{aligned}
\tag{2}
$$

The minimization of $J(u, v^{(n-1)})$ with respect to u can be done by means of an iterative thresholding algorithm [14]. The minimizer $v^{(n)}$ of $J(u^{(n)}, v)$ for fixed $u^{(n)}$ can be computed explicitly. Indeed, it follows from elementary calculus that

$$
v_\lambda^{(n)} = \begin{cases} \rho_\lambda - \frac{1}{2\theta_\lambda}\|u^{(n)}\lambda\|_q & \text{if } \|u^{(n)}\lambda\|_q < 2\theta_\lambda\rho_\lambda \\ 0 & \text{otherwise .} \end{cases}
\tag{3}
$$

We have the following result about the convergence of the above algorithm.

Theorem 1. *Assume $q \in \{1, 2, \infty\}$ and $\theta_\lambda\omega_\lambda \geq \sigma > \phi_q/4$ for all $\lambda \in \Lambda$, where $\phi_1 = M$, $\phi_2 = 1$, $\phi_\infty = \sqrt{M}$. Moreover, we assume that $\omega_\lambda \geq \gamma > 0$ for all $\lambda \in \Lambda$. Then the sequence $(u^{(n)}, v^{(n)})_{n \in \mathbb{N}}$ converges to the unique minimizer $(u^*, v^*) \in \ell_2(\Lambda, \mathbb{R}^M) \times \ell_{\infty,\rho^{-1}}(\Lambda)_+$ of J. The convergence of $u^{(n)}$ to u^* is strong in $\ell_2(\Lambda, \mathbb{R}^M)$ and $v^{(n)} - v^*$ converges to 0 strongly in $\ell_{2,\theta}(\Lambda)$.*
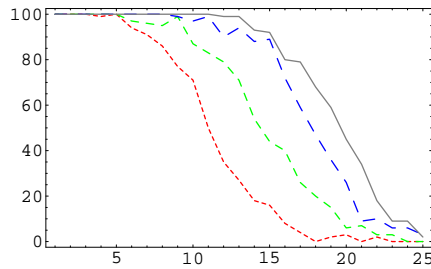

Fig. 3. In ordinate we illustrate the probability of exact support recovery from a fixed number of random linear measurements. In abscissa we illustrate the size of the support to be reconstructed. The different curves represent the probability of reconstruction for increasing number $M = 2, 4, 8, 16$ of channels under joint sparsity constraints, from the most dashed to the solid one. The fidelity of the reconstruction increases with the number of channels.

2.3 Fidelity in Joint Sparse Recovery

We want to discuss the effect of the coupling due to joint sparsity for the fidelity of the reconstruction. Let us assume that $M = N$, the matrices $T_{\ell,j} = 0$ for $j \neq \ell$, and $T_{\ell,\ell}$ are generic matrices, *i.e.*, random matrices with zero mean i.i.d. Gaussian entries. This means that we do not consider at the moment either a specific color model or a particular color datum. We only assume that the color

channels are coupled in terms of sparsity. This situation appears previously in the literature under the name of *distributed compressed sensing*, see [2]. Since random matrices have, "with overwhelming probability", the so-called *Restricted Isometry Property* (see [5, 6] for details), it is essentially sufficient to recover the location of the non-zero coefficients u_λ^ℓ in order to recover their value too. Applications of our joint sparsity algorithm (2) show that the probability of perfect reconstruction of the support of u increases with the number of channels M, see Fig. 3, see also [2]. The moral is that it is more probable the faithful reconstruction of a color image encoded into multiple channels as soon as we couple the channels in terms of their sparsity, which, in turn, means coupling derivatives. This further explains the positive results obtained in the papers [22, 29].

3 Restoration of Vector Valued BV Functions from Projections

The gray level can be also interpreted as a combination of the color (*e.g.*, RGB) intensities to impose, besides derivatives, an additional constraint to fidelity. In this section we want to recall the model proposed by the author in [17, 18] and to discuss its fidelity. In this recolorization model, the color image is encoded into RGB channels and no coupling of derivatives is explicitly imposed. This situation is opposite to the one previously discussed, where no coupling was claimed with respect to data instead.

A digital image can be modeled as a function $u : \Omega \subset \mathbb{R}^2 \to \mathbb{R}^3_+$, so that, to each "point" x of the image, one associates the vector $u(x) = (r(x), g(x), b(x)) \in \mathbb{R}^3_+$ of the color represented by the different channels red, green, and blue. The gray
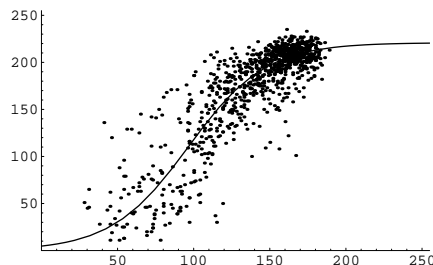

Fig. 4. Estimate of the nonlinear curve L from a distribution of points with coordinates given by the linear combination $\alpha r + \beta g + \gamma b$ of the (r, g, b) color fragments (abscissa) and by the corresponding underlying gray level of the original photographs dated to 1920 (ordinate). The sensitivity parameters α, β, γ to the different frequencies of red, green, and blue are chosen in order to minimize the total variance of the ordinates. However, it is always possible to re-equalize the gray level to make $\mathcal{L}(r, g, b) = \frac{1}{3}(r, g, b)$.

level of an image can be described as $\mathcal{L}(r, g, b) := L(\alpha r + \beta g + \gamma b), (r, g, b) \in \mathbb{R}^3_+$,

where $\alpha, \beta, \gamma > 0$, $\alpha + \beta + \gamma = 1$, $L : \mathbb{R} \to \mathbb{R}$ is a non-negative increasing function, see Fig. 4. The recolorization is modeled as the minimum solution of the functional

$$
F(u) = \mu \underbrace{\int_{\Omega \setminus D} |u(x) - \bar{u}(x)|^p dx}_{=G_1(u)} + \lambda \underbrace{\int_D |\mathcal{L}(u(x)) - \bar{v}(x)|^p dx}_{=G_2(u)} + \int_\Omega \sum_{\ell=1}^M |\nabla u^\ell(x)| dx,
$$

(4)

where we want to reconstruct the vector valued function $u := (u^1, \dots, u^M) : \Omega \subset \mathbb{R}^d \to \mathbb{R}^M$ ($M = 3$ for RGB images) from a given observed couple of color/gray level functions $(\bar{u}, \bar{v})$. Without loss of generality let us assume $\lambda = \mu = 1$. For the computation of minimizers, we use a similar approach as in (2). For simplicity we assume $d = p = 2$. Let us introduce a new functional given by

$$
\mathcal{E}_h(u, v) := 2 \left(G_1(u) + G_2(u) \right) + \int_\Omega \sum_{\ell=1}^M \left(v^\ell |\nabla u^\ell(x)|^2 + \frac{1}{v^\ell} \right) dx,
$$

(5)

where $u \in W^{1,2}(\Omega; \mathbb{R}^M)$, and $v \in L^2(\Omega; \mathbb{R}^M)$ is such that $\varepsilon_h \leq v^\ell \leq \frac{1}{\varepsilon_h}$, $\ell = 1, \dots, M$, $\varepsilon_h \to 0$ for $h \to \infty$. While the variable u is again the function to be reconstructed, we call the variable v the *gradient weight*. For any given $v^{(0)} \in L^2(\Omega; \mathbb{R}^M)$ (for example $v^{(0)} := 1$), we define the following iterative double-minimization algorithm:

$$
\begin{cases}
u^{(n+1)} = \arg \min\limits_{u \in W^{1,2}(\Omega; \mathbb{R}^M)} \mathcal{E}_h(u, v^{(n)}) \\
v^{(n+1)} = \arg \min\limits_{\varepsilon_h \leq v \leq \frac{1}{\varepsilon_h}} \mathcal{E}_h(u^{(n+1)}, v).
\end{cases}
$$

(6)

We have the following convergence result.

Theorem 2. *The sequence $\{u^{(n)}\}_{n \in \mathbb{N}}$ has subsequences that converge strongly in $L^2(\Omega; \mathbb{R}^M)$ and weakly in $W^{1,2}(\Omega; \mathbb{R}^M)$ to a point $u_h^{(\infty)}$. We have that $(u_h^{(\infty)})_h$ converges for $h \to \infty$ in $BV(\Omega; \mathbb{R}^M)$ to a stationary point of the Euler-Lagrange equations of F.*

3.1 Fidelity in Linear Projection Method

We want to highlight the relations between the models (4) and (1), with particular emphasis on the fidelity of reconstruction. For the sake of simplicity we consider 1D *discrete* signals, *i.e.* $d = 1$, and a linear projection $\mathcal{L}(x_1, \dots, x_M) = \frac{1}{M}(x_1, \dots, x_m)$. The set $\Omega = \{0, 1, \dots, \omega - 1\}$, for $\omega := |\Omega| > 0$. For a discrete signal of length ω, we define the total variation as follows. Let us denote with $\mathcal{D}$ the $(\omega - 1) \times \omega$ *derivative matrix*

$$
\mathcal{D} := \begin{pmatrix}
-1 & 1 & 0 & \dots & 0 & 0 \\
0 & -1 & 1 & \cdots & 0 & 0 \\
\dots & \dots & \dots & \dots & \dots & \dots \\
0 & 0 & 0 & \cdots & -1 & 1
\end{pmatrix}.
$$

(7)

Fig. 5. The first column illustrates two different data for the recolorization problem. The second column illustrates the corresponding 10th iteration algorithm (6). In the bottom-left position we illustrate a datum with only the 3% of original color information, randomly distributed.

The discrete total variation of $v = (v_0, \ldots, v_{\omega-1})^T$ is given by

$$TV(v) := \|\mathcal{D}v\|_1 = \sum_{m=1}^{\omega-1} |(\mathcal{D}v)_m|.$$

The discrete version of (4) reads

$$F_d(u) = \mu \sum_{n \in \Omega \setminus D} |u_n - \bar{u}_n|^2 + \lambda \sum_{n \in D} |\mathcal{L}(u_n) - \bar{v}_n|^2 + \underbrace{\sum_{\ell=1}^{M} \sum_{m=1}^{\omega-1} |(\mathcal{D}u^\ell)_m|}_{\text{TV-constraint}}. \qquad (8)$$

Observe that the total variation constraint is now re-formulated as a *sparsity constraint* on the derivative. Let us first analyze the model with no noise, *i.e.*, for $\lambda, \mu \to \infty$, the minimization problem becomes

$$\min \sum_{\ell=1}^{M} \sum_{m=1}^{\omega-1} |(\mathcal{D}u^\ell)_m| \text{ subject to } Gu = (\bar{u} \quad \bar{v})^T, \qquad (9)$$

where

$$
G := \begin{pmatrix}
I_{\Omega \setminus D} & 0 & 0 & \dots & 0 & 0 \\
0 & I_{\Omega \setminus D} & 0 & \cdots & 0 & 0 \\
\cdots & \cdots & \cdots & \cdots & \cdots & \cdots \\
0 & 0 & 0 & \cdots & 0 & I_{\Omega \setminus D} \\
\frac{1}{M} I_D & \frac{1}{M} I_D & \cdots & \cdots & \cdots & \frac{1}{M} I_D
\end{pmatrix}.
$$

Let us denote $f := (\bar{u} \quad \bar{v})^T$. We have the following result.

Lemma 1. *We assume that the signal u to be reconstructed is consistent, i.e. $Gu = f$, and with joint sparse derivative,*

$\mathrm{supp}(\mathcal{D}u^\ell) \subset \mathrm{supp}(\mathcal{D}\mathcal{L}(u)), \quad \ell = 1, \dots, M, \text{ where } |\mathrm{supp}(\mathcal{D}\mathcal{L}(u))| = K \leq \omega - 1.$

Then the solution u^* to (9) necessarily has the property

$$
\mathrm{supp}(\mathcal{D}(u^*)^\ell) \subset \mathrm{supp}(\mathcal{D}\mathcal{L}(u)), \quad \ell = 1, \dots, M.
$$

Proof. Let us consider the derivative of the solution u^*, we have

$$
\frac{1}{M} \sum_{\ell=1}^{M} \mathcal{D}(u^*)_m^\ell = 0, \quad m \in \{1, \dots, \omega - 1\} \setminus \mathrm{supp}(\mathcal{D}\mathcal{L}(u)).
$$

If we assumed $\mathcal{D}(u^*)_m^\ell \neq 0$ then we would increase $\sum_\ell TV((u^*)^\ell)$. Since we minimize the total variation and the choice $\mathcal{D}(u^*)_m^\ell = 0$ does not spoil the consistency with the data, necessarily $\mathcal{D}(u^*)_m^\ell = 0$.

Remark 1. This lemma applied to this simplified model essentially tells that, by coupling the color channels to match the gray level (here reproduced as a linear combination of the colors) and by minimizing at the same time the sum of the total variations of each individual channel, we necessarily obtain a coupling of the derivatives of the solution. Therefore, although it is not explicitly required by the formulation of the constraints, this second model produces the same effect of coupling derivatives as the first one. This explains why also this model is very effective in recolorization, see examples in [18].

We want now to address more specifically the problem of fidelity. In Fig. 5 we show two examples of applications of algorithm (6) depending on two different initial configurations of the color datum. It is clear that few uniformly distributed samples of color are more representative than lots of samples only locally distributed. We formalize this observation in the following proposition.

Proposition 1. *We assume that the signal u to be reconstructed is consistent, i.e. $Gu = f$, and with joint sparse derivative,*

$\mathrm{supp}(\mathcal{D}u^\ell) \subset \mathrm{supp}(\mathcal{D}\mathcal{L}(u)), \quad \ell = 1, \dots, M, \text{ where } |\mathrm{supp}(\mathcal{D}\mathcal{L}(u))| = K \leq \omega - 1.$

This means that the signal u is piecewise constant. For

$$
\mathcal{J} := \{I \subset \Omega : I \text{ is an interval and } u|_I \text{ is constant } \},
$$

we also assume that $(\Omega \setminus D) \cap I \neq \emptyset$ for all $I \in \mathcal{J}$ and, without loss of generality, $0 \in (\Omega \setminus D)$. Then the solution u^* to (9) necessarily coincides with u.

Proof. We sketch the proof of the proposition. Let us consider the $\omega \times (\omega - 1)$ *integration matrix*

$$\mathcal{I} := \begin{pmatrix} 0 & 0 & 0 & \dots & 0 & 0 \\ 1 & 0 & 0 & \cdots & 0 & 0 \\ 1 & 1 & 0 & \cdots & 0 & 0 \\ \dots & \dots & \dots & \dots & \dots & \dots \\ 1 & 1 & 1 & \cdots & 1 & 1 \end{pmatrix}.$$

We have $\mathcal{DI} = I_{(\omega-1)\times(\omega-1)}$ and $v = \mathcal{ID}v + C_v$ for all $v \in \mathbb{R}^\omega$, where $C_v = (c_v, \dots, c_v)$ is a constant. Then for $z = (\mathcal{D}u^\ell)_{\ell=1}^M$, (9) can be equivalently reformulated as

$$\min \sum_{\ell=1}^M \sum_{m=1}^{\omega-1} |z_m^\ell| \text{ subject to } \tilde{G}z = f - \tilde{f}_z, \tag{10}$$

where $\tilde{f}_z := (I_{\Omega \setminus D} C_{z^1}, \dots, I_{\Omega \setminus D} C_{z^M}, \frac{1}{M} \sum_{\ell=1}^M I_D C_{z^\ell}, \dots, \frac{1}{M} \sum_{\ell=1}^M I_D C_{z^\ell})^T$. The constants $c_{z^\ell} = u_0^\ell$ for all $\ell = 1, \dots, M$. Moreover, by Lemma 1 we know already that $\text{supp}(z^\ell) \subset \text{supp}(\mathcal{DL}(u)) := T, \quad \ell = 1, \dots, M$. It is sufficient now to observe that $(I_{\Omega \setminus D}\mathcal{I})|_T$ is necessarily a full rank matrix and $\tilde{G}z = f - \tilde{f}_z$ has a unique solution z^*. Therefore, we have $u^* = \mathcal{I}z^* + C_{z^*} = u$.

Of course, to model images as piecewise constant functions is quite unrealistic. We may better model u as belonging to the class of signals with (K, ε)-sparse derivatives defined by $S_{\varepsilon,K} := \{u \in \mathbb{R}^{\omega \times M} : \#\{m : |\mathcal{D}u_m^\ell| > \varepsilon\} \le K\}$, for $\varepsilon > 0$ and $K \le \omega - 1$. If an *oracle* could tell us that $\{m : |\mathcal{D}u_m^\ell| > \varepsilon\} \subset T$, for a fixed $T \subset \Omega$, for all $\ell = 1, \dots, M$ and $(\Omega \setminus D) \cap I \ne \emptyset$ for each interval $I = [a, b] \subset \Omega$ such that $\partial I = \{a, b\} \subset T$, but $(I \setminus \partial I) \cap T = \emptyset$, then again $(I_{\Omega \setminus D}\mathcal{I})|_T$ would be a full rank matrix and we could easily compute u_ε^* such that $\|u_\varepsilon^* - u\|_2 \le C\varepsilon$, for a constant $C = C(\omega; K)$ independent of u and ε. One may argue that this oracle can be furnished directly by the gray level, *e.g.*, by segmentation. Nevertheless, although the matrices $\tilde{G}$ do not have the Restricted Isometry Property, numerical experiments indicate that such an oracle is indeed directly provided by the support of the derivative of the minimizer u_ε^* of (8), for suitable constants $\lambda(\varepsilon), \mu(\varepsilon) > 0$. Moreover, such minimizers do already satisfy the property $\|u_\varepsilon^* - u\|_2 \le C\varepsilon$.

References

1. Ballester, C., Bertalmio, M., Caselles, V., Sapiro, G., and Verdera, J.: *Filling-in by joint interpolation of vector fields and gray levels.*, IEEE Trans. Image Process. **10** (2001), no. 8, 1200–1211.
2. Baron, D., Wakin, M. B., Duarte, M. F., Sarvotham S., and Baraniuk R G.: *Distributed compressed sensing*, preprint (2005).
3. Beltramio, M., Sapiro, G., Caselles, V., and Ballester, B.: *Image inpainting*, SIGGRAPH 2000, 2001.
4. Candès, E. J. and Donoho, D. L.: *New tight frames of curvelets and optimal representations of objects with piecewise C^2 singularities.*, Commun. Pure Appl. Math. **57** (2004), no. 2, 219–266.

5. Candès, E. J., Romberg, E.J., and Tao, J.: *Exact signal reconstruction from highly incomplete frequency information*, IEEE Trans. Inf. Theory **52** (2006), no. 2, 489–509.

6. Candès, E. J, Romberg, E.J., and Tao, T.: *Stable signal recovery from incomplete and inaccurate measurements*, preprint (2005).

7. Caselles, V.,Coll, V., and Morel, J.-M.: *Geometry and color in natural images*, Journal of Mathematical Imaging and Vision, **16** (2002) no. 2 89–105.

8. Cazzato R., Costa G., Dal Farra A., Fornasier M., Toniolo D., Tosato D., and Zanuso C.: *Il Progetto Mantegna: storia e risultati* (Italian), in "Andrea Mantegna e i Maestri della Cappella Ovetari: La Ricomposizione Virtuale e il Restauro" (Eds. Anna Maria Spiazzi, Alberta De Nicolò Salmazo, Domenico Toniolo), Skira, 2006.

9. Chan, T. F. and Kang, S. H.: *Error analysis for image inpainting*, UCLA CAM 04-72, (2004).

10. Chan, T. F. and Kang, S. H. and Shen, J.: *Euler's elastica and curvaure-based inpainting*, SIAM J. Appl. Math. **63** (2002), no. 2, 564–592.

11. Chan, T. F. and Shen, J.: *Inpainting based on nonlinear transport and diffusion*, Contemp. Math. **313** (2002), 53–65.

12. Chan, T. F. and Shen, J.: *Mathematical models for local nontexture inpaintings*, SIAM J. Appl. Math. **62** (2002), no. 3, 1019–1043.

13. Chan, T. F. and Shen, J.: *Variational image inpainting*, Commun. Pure Appl. Math. **58** (2005), no. 5, 579–619.

14. Daubechies, I., Defrise M. and DeMol, C.: *An iterative thresholding algorithm for linear inverse problems*, Comm. Pure Appl. Math. **57** (2004), no. 11, 1413–1457.

15. Donoho, D. L.:*Compressed Sensing*, IEEE Trans. Inf. Theory **52** (2006), no. 4, 1289–1306.

16. Elad, M.,Starck, J.-L.,Querre, P., and Donoho, D.L.,: *Simultaneous cartoon and texture image inpainting using morphological component analysis (MCA)*, Appl. Comput. Harmon. Anal. **19** (2005), 340–358.

17. Fornasier M.: *Nonlinear projection recovery in digital inpainting for color image restoration*, J. Math. Imaging Vis. **24** (2006), no. 3, 359–373.

18. Fornasier M. and March R.: *Restoration of color images by vector valued BV functions and variational calculus*, Johann Radon Institute for Computational and Applied Mathematics (RICAM) preprint 2006-30 (2006).

19. Fornasier M. and Rauhut H.: *Recovery algorithms for vector valued data with joint sparsity constraints*, Johann Radon Institute for Computational and Applied Mathematics (RICAM) preprint 2006-27 (2006).

20. Fornasier M. and Toniolo D.: *Computer-based recomposition of the frescoes in the Ovetari Chapel in the Church of the Eremitani in Padua. Methodology and initial results, (English/Italian)*, in "Mantegna nella Chiesa degli Eremitani a Padova. Il recupero Possibile", Ed. Skira, 2003.

21. Fornasier M. and Toniolo D.: *Fast, robust, and efficient 2D pattern recognition for re-assembling fragmented digital images*, Pattern Recognition **38** (2005), 2074–2087.

22. Kang, S. H. and March, R.: *Variational models for image colorization via Chromaticity and Brightness decomposition*, preprint (2006).

23. Levin, A., Lischinski, A. and Weiss Y,: *Colorization using optimization*, Proceedings of the 2004 SIGGRAPH Conference, **23** (2004) no. 3 689–694.

24. Mallat, S.: *A Wavelet Tour of Signal Processing. 2nd Ed.*, San Diego, CA: Academic Press., 1999.

25. Masnou, S.: *Filtrage et Désocclusion d'Images par Méthodes d'Ensembles de Niveau*, PhD Thesis, Université Paris-Dauphine (1998).

26. Masnou, S.: *Disocclusion: a variational approach using level lines*, IEEE Trans. on Image Processing, **11** 68–76, no. 2 68–76

27. Masnou S. and Morel J.-M.:, *Level lines based disocclusion.* Proceedings of 5th IEEE IEEE Intl Conf. on Image Process.,Chicago, **3** (1998) 259–263.

28. Mumford, D.: *Elastica and computer vision*, Algebraic geometry and applications, ed. C. Bajaj, Springer-Verlag, Heidelberg, (1994) 491–506.

29. Sapiro G.: *Inpainting the colors*, ICIP 2005. IEEE International Conference on Image Processing, **2** (2005), 698–701.

30. Tropp, J.: *Algorithms for simultaneous sparse approximation. Part II: Convex relaxation*, Signal Processing **86** (2006), 589–602.

31. Yatziv, L. and Sapiro, G.: *Fast image and video colorization using chrominance blending*, IEEE Transactions on Image Processing **15** (2006), no. 5, 1120–1129.